Summertime runoff variations and their connections with Asian summer monsoons in the Yangtze River basin

Jian Tang, Qingyun Li and Jin Chen

ABSTRACT

Research on the summertime runoff variations and their connections with Asian summer monsoons can give insights for explanation of the hydrological processes and climate change in the Yangtze River basin. Currently, regional studies are focused on the relationships between Asian summer monsoons and meteorological elements. However, research on the runoff variations and their connections to Asian summer monsoons is still scarce. With the help of continuous wavelet transform, cross-wavelet, and wavelet coherence analysis methods, this research explored multiscale summertime runoff variations and their connections with Asian summer monsoons during 1957–2012 in the Yangtze River basin. The results indicate that periodical characteristics of summertime runoff along the mainstream of the Yangtze River basin have distinct differences. Upstream flow is characterized by interannual (1- to 3-year), and downstream by decadal (7- to 10-year) oscillations over certain time periods. In the source region, summertime runoff is primarily influenced by the South Asian summer monsoons (SASM), and mainly in-phase relationships are detected between the summertime runoff and SASM indices. In the midstream and downstream regions, summertime runoff is primarily influenced by the East Asian summer monsoons (EASM), and mainly anti-phase relationships are detected between the summertime runoff and EASM indices.

Key words | Asian summer monsoons, continuous wavelet transform, cross-wavelet and wavelet coherence analysis, summertime runoff, Yangtze River basin

Jian Tang
Qingyun Li
Jin Chen (corresponding author)
Basin Water Environmental Research Department,
Changjiang River Scientific Research Institute,
Wuhan 430010,
China
and
Key Laboratory of Basin Water Resource and Eco-environmental Science in Hubei Province,
Changjiang River Scientific Research Institute,
Wuhan 430010,
China
E-mail: *chenjincrsri@163.com*

INTRODUCTION

Monsoons are important heat conveyors and rain-bearing systems, running from the tropics to the middle latitudes in the Northern Hemisphere (Kulkarni *et al.* 2012; Kurita *et al.* 2015). Asian summer monsoons are one of the strongest elements of the global monsoon system, and form as a result of thermal differences between the Asian landmass and the Pacific Ocean (Lee *et al.* 2013; Singh *et al.* 2014). More than 60% of the world's population depends on Asian summer monsoon rainfall. Asian summer monsoons play a crucial role in providing water resources for agriculture, industrial development, and basic human needs (Turner & Annamalai 2012; Wu *et al.* 2012). In recent decades, researchers have been paying increasing attention to the linkages between runoff and Asian summer monsoons in river basins (Schiemann *et al.* 2007; Wei *et al.* 2014; Latt & Wittenberg 2015; Li *et al.* 2017). Such research could give insights into the effects of climate change on hydrological processes. These research topics are therefore essential for assisting water managers in developing sustainable water resource management and protection (Thomas *et al.* 2015; Gebregiorgis *et al.* 2016; Steirou *et al.* 2017).

Asian summer monsoons are critical to the global transport of atmospheric energy and water vapor. In central and southern Asia, a significant contemporaneous relationship between summer runoff and the intensity of the Asian summer monsoons has been observed (Schiemann *et al.* 2007). In the interiors of India and China, South Asian and East Asian summer monsoons introduce the majority

doi: 10.2166/wcc.2017.142

of annual precipitation by seasonal storms or floods, which in turn influence regional hydrological processes (Clift *et al.* 2008). At approximately 6,380 km, Yangtze River is the longest river in Asia and the third longest river in the world (Yang *et al.* 2006). Asian summer monsoons are also the heat conveyors and rain-bearing systems of the Yangtze River basin. The monsoons influence the runoff in the Yangtze River basin (Blender *et al.* 2011; Zeng *et al.* 2014; Kubota *et al.* 2015). Therefore, research topics that clarify the linkages between runoff and Asian summer monsoons need to be addressed in the Yangtze River basin (Cuo *et al.* 2014; Li *et al.* 2016).

Asian summer monsoon changes and the induced runoff variations directly affect the lives of people and animals that depend on the Yangtze River. Therefore, the runoff variations and their links to Asian summer monsoons in the Yangtze River basin have attracted much attention. Over the last few decades, many efforts have been made to study the relationships between Asian summer monsoons and meteorological elements in the Yangtze River basin (Li *et al.* 2016). Zhang *et al.* (2008) investigated spatial and temporal variations of the precipitation maxima and their relationships with Asian summer monsoons in the Yangtze River basin. Han *et al.* (2015) explored the multiscale trends in precipitation extremes and the possible links with monsoon indices. Shan *et al.* (2017) explored the evolution characteristics of dry-wet abrupt alternation and its connections with Asian summer monsoons in the middle and lower reaches of the Yangtze River Basin. This research is helpful for understanding and controlling flood and drought problems in the Yangtze River basin. However, research on the runoff variations and its connections to Asian summer monsoons in the Yangtze River basin is still lacking (Li *et al.* 2016). Therefore, it is essential to explore the runoff variations and their connections to Asian summer monsoons in the Yangtze River basin. Research results can assist water managers in developing a sustainable water resource management strategy.

Taking summertime runoff in the Yangtze River basin as a case study, the aim of this study is to explore the characteristics of summertime runoff and Asian summer monsoon variations and detect the multiscale relationships between summertime runoff and Asian summer monsoons in the sub-regions of the Yangtze River basin.

STUDY AREA

The Yangtze River originates from a glacier in Geladandong Peak in Western China. The river has a total length of approximately 6,300 km and a drainage basin of 1,800,000 km^2. It wanders through 11 provinces and autonomous regions, and finally discharges into the Yellow Sea and East China Sea at Shanghai. Zhimenda hydrological station is the last national-level station located in the source region of the Yangtze River basin. Yichang hydrological station is located at the upper reaches of the Yangtze River basin. Hankou hydrological station, located at the midstream section, is the key reference station for flood mitigation and flood control in the basin (Yang *et al.* 2006). Datong hydrological station is the last hydrological station that is unaffected by tides located downstream of the Yangtze River basin (Table 1) (Zhang *et al.* 2012). Therefore, these four hydrological stations are selected to represent the source, upper, middle, and lower reaches of the river basin (Figure 1).

DATA ACQUISITION AND PROCESSING

Monthly runoff data of the selected stations were collected from the hydrological yearbooks of China. Runoff data were quality controlled, and provide a continuous record from 1957 to 2012. Summertime runoff data of Zhimenda, Yichang, Hankou, and Datong hydrological stations are used in this research. Summertime runoff data is the average runoff over the summer months of June, July and August.

The Asian summer monsoons are composed of two subsystems, East Asian summer monsoon (EASM) and South Asian summer monsoon (SASM) (Wang & Zhou 2005). Indices of the EASM and SASM are therefore used to

Table 1 | Details about the selected hydrological stations

Stations	Longitude	Latitude	Elevation (m)	Drainage area (km^2)
Zhimenda	97°13′	33°02′	3,560	137,704
Yichang	111°17′	30°42′	86	1,005,501
Hankou	114°17′	30°35′	20	1,488,036
Datong	117°37′	30°46′	9	1,725,000

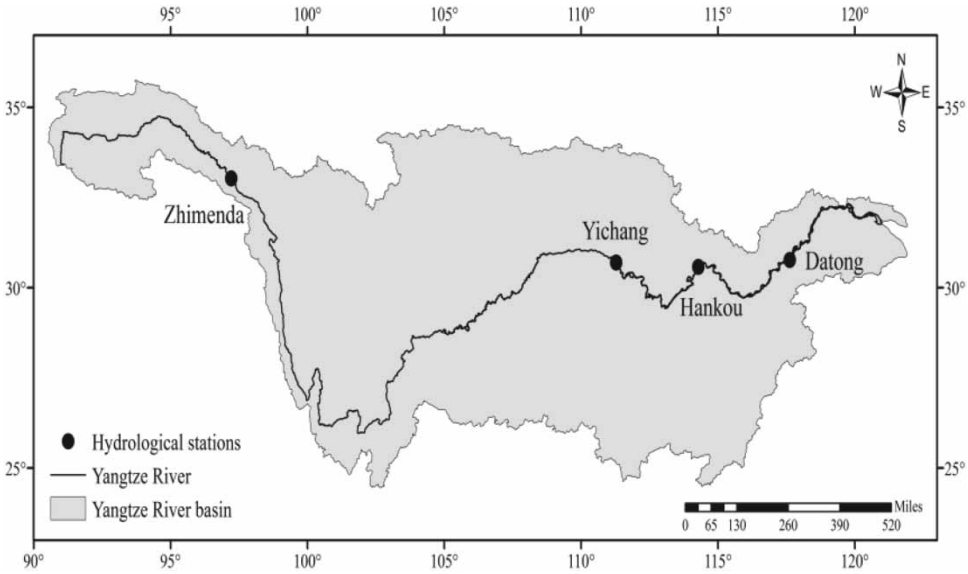

Figure 1 | Sketch map of the study area.

characterize the Asian summer monsoon's changes. The EASM index is defined as an area-averaged seasonally meridional wind at 850 hPa within the East Asian monsoon domain (10–40°N, 110–140°E). The SASM index is defined as an area-averaged seasonally zonal wind at 850 hPa within the South Asian domain (5–22.5°N, 35–97.5°E) (Li & Zeng 2002; Li *et al.* 2010). EASM and SASM indices were collected from http://www.lasg.ac.cn/staff/ljp.

METHODS

Continuous wavelet transform

Continuous wavelet transform can be used to analyze time series at many different frequencies. It can clearly describe the dominant modes of variation in a hydrological time series (Sang 2013).

The basic idea of continuous wavelet transform is the decomposition of $f(t)$ in a set of $\psi_{a,b}(t)$ functions:

$$W_f(a,b) = |a|^{-\frac{1}{2}} \int_{-\infty}^{\infty} f(t)\psi^*_{a,b}(t)dt \quad (1)$$

where $W_f(a,b)$ denotes the continuous wavelet transforms of $f(t)$ at scales a and positions b. $\psi_{a,b}(t)$ is derived through contraction and expansion of the mother wavelet $\psi(t)$.

In this research, the complex Morlet wavelet was used as the mother wavelet. The complex Morlet wavelet is non-orthogonal and complex:

$$\psi(t) = e^{iw_0 t} e^{\frac{-t^2}{2}} \quad (2)$$

where w_0 is the non-dimensional frequency; in this study, w_0 is set at 6 to satisfy the admissibility condition (Fourier transform of the mother wavelet can satisfy $\int_{-\infty}^{\infty} \frac{|\psi(\omega)|^2}{\omega} d\omega < +\infty$) (Farge 1992).

Cross-wavelet and wavelet coherence analysis

Cross-wavelet and wavelet coherence analysis are powerful methods for testing potential linkages between two time series at multiple time scales (Labat 2005; Ionita *et al.* 2012; Tamaddun *et al.* 2017).

Assume that there are two time series x and y; a cross-wavelet power is defined to identify correlation between the two time series using the product of their wavelet coefficients (Adamowski & Prokoph 2014). The cross-wavelet

spectra for the two time series can be defined as:

$$C_{xy}(a, b) = S(C_x^*(a, b)C_y(a, b)) \tag{3}$$

Wavelet coherence is a measure of the intensity of the covariance of the two series in time-frequency space. The wavelet coherence of the two time series can be defined as:

$$\frac{SC_x^*(a, b)C_y(a, b)}{\sqrt{S\left(|C_x(a, b)|^2\right)}\sqrt{S\left(|C_y(a, b)|^2\right)}} \tag{4}$$

where $C_x(a,b)$ and $C_y(a,b)$ denote the continuous wavelet transforms of x and y, respectively. The superscript * is the complex conjugate, and S is a smoothing operator in time and scale. For details about how to design the smoothing operator for the Morlet wavelet, refer to Torrence & Webster (1998).

In this research, the relationships between summertime runoff and Asian summer monsoons indices are explored by cross-wavelet and wavelet coherence analysis methods. The statistical significance of the cross-wavelet spectrum is estimated against a red noise model (Torrence & Compo 1998), and the statistical confidence level of the wavelet coherence spectrum is determined by a Monte Carlo method (Grinsted *et al.* 2004). The thick black contour in the power spectra designates the 95% confidence level against red noise, and areas outside the cone of influence where edge effects might distort the picture are shown in lighter shades.

RESULTS

Summertime runoff variations in the Yangtze River basin

Multi-scale variation characteristics of summertime runoff along the mainstream of the Yangtze River are explored by continuous wavelet transform. Figure 2 illustrates the

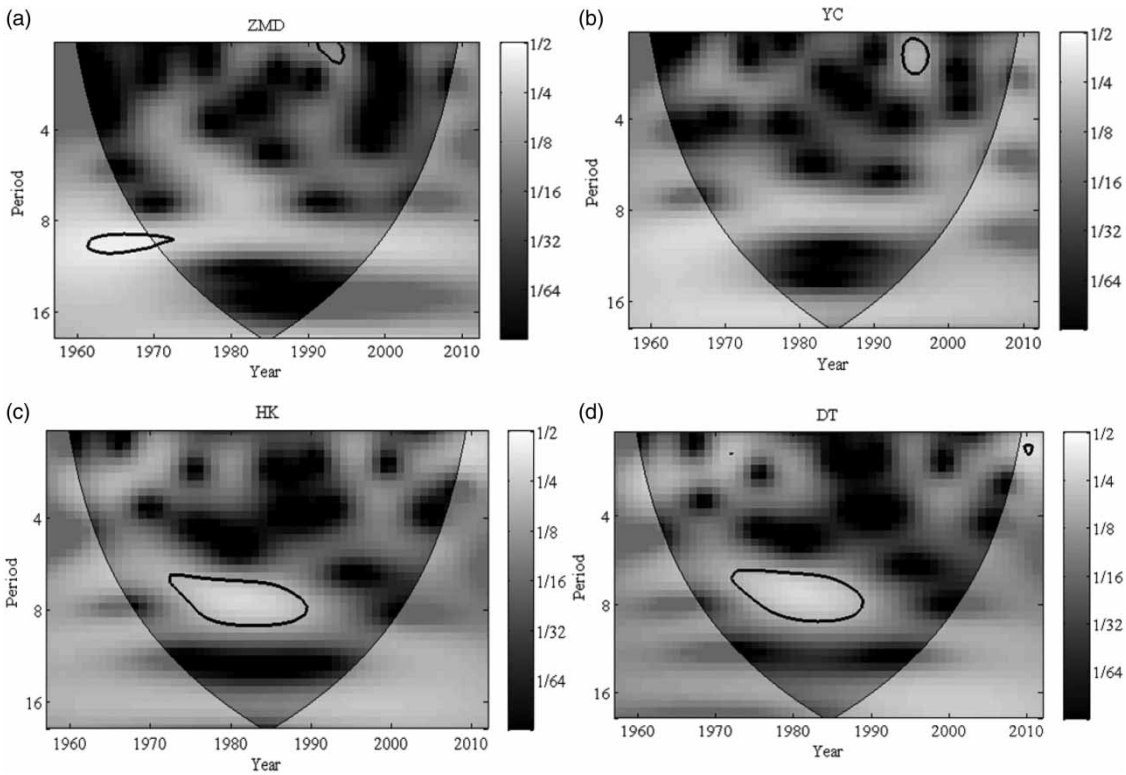

Figure 2 | Wavelet power spectra of summertime runoff in the Yangtze River basin during 1957–2012: (a) Zhimenda hydrological station; (b) Yichang hydrological station; (c) Hankou hydrological station; and (d) Datong hydrological station.

power spectra of normalized summertime runoff during 1957–2012. The significant wavelet power spectra of summertime runoff at Zhimenda hydrological station are in the 1- to 2-year band around 1991–1995, and in the 9- to 10-year band around 1970–1974 (Figure 2(a)). The significant wavelet power spectra of summertime runoff at Yichang hydrological station (Figure 2(b)) show high wavelet power in the 1- to 3-year band around 1991–1995. Summertime runoffs at Zhimenda and Yichang hydrological stations have common features. A high wavelet power in the 1- to 2-year band around 1991–1995 was detected in the wavelet power spectra. The power spectra of summertime runoff at Hankou hydrological station are shown in Figure 2(c). The significant wavelet power spectra show high wavelet power in the 7- to 10-year band around 1972–1990. Similar periodic characteristics were also detected at Datong hydrological station (Figure 2(d)).

Summer runoff variation characteristics have distinct differences between the upper and lower reaches of the Yangtze River (Wei *et al.* 2014). For the Zhimenda and Yichang stations located in the upper reaches, high wavelet power in the 1- to 3-year band is detected in the wavelet power spectra for average annual summer runoff around 1991–1995. In the Hankou and Datong hydrological stations located in the lower reaches, high wavelet power in the 7- to 10-year band is detected in the wavelet power spectra for average annual summer runoff around 1972–1990.

Variations of Asian summer monsoon indices

Multi-scale variation characteristics of the Asian summer monsoon indices during 1957 to 2012 were also explored by continuous wavelet transform. The power spectra of normalized EASM and SASM indices are shown in Figure 3. High wavelet power in the 1- to 3-year band is identified in the power spectra of EASM indices around 1979–1984 and 1995–2001 (Figure 3(a)). For the SASM, the significant wavelet power spectra show high wavelet power in the 1- to 6-year band around 1965–1980 and 1986–1996 (Figure 3(b)). After 1990, the EASM and SASM indices have similar periodic characteristics (high wavelet power in the 1- to 3-year band) as the summertime runoff at Zhimenda and Yichang hydrological stations. There are no similarities in the periodic characteristics between Asian summer monsoon indices and summertime runoff at Hankou and Datong hydrological stations. The EASM and SASM exhibit approximately a 2-year dominant periodicity (Ding *et al.* 2013). However, summertime runoff of Hankou and Datong hydrological stations has a long-term periodicity (Figure 2(c) and 2(d)). These results indicate that the Asian summer monsoons have close relationships with summertime runoff at the source and upper regions of the Yangtze River basin (Kitoh 2004; Ding & Chan 2005; Zhang *et al.* 2008).

Connections between summer runoff and Asian summer monsoons

To elaborate the multi-scale relationships between Asian summer monsoons and summertime runoff in the Yangtze River basin, cross-wavelet analysis and wavelet coherence analysis methods are applied to detect the linkages between the two time series.

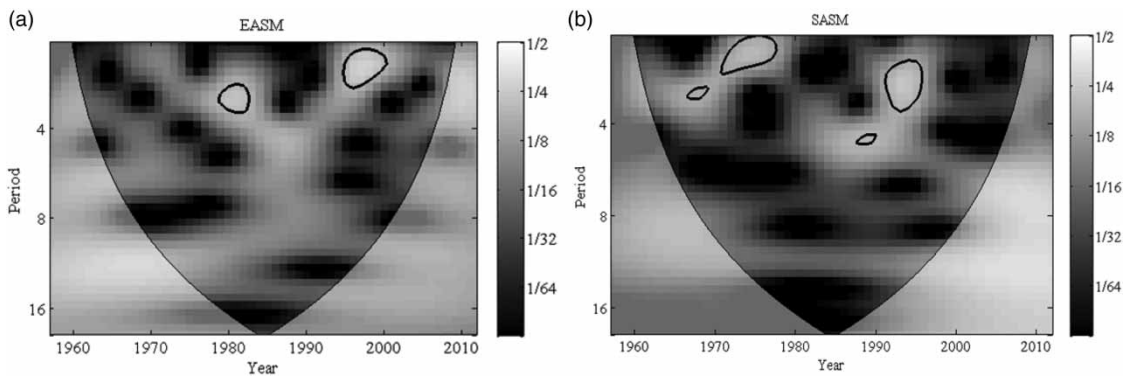

Figure 3 | Wavelet power spectra of Asian summer monsoon indices during 1957–2012: (a) EASM; (b) SASM.

In the source region of the Yangtze River basin, cross-wavelet power spectra of summertime runoff and EASM indices show high power in the 1- to 3-year band around 1991–1995 and the 10- to 11-year band around 1970–1972. The 1- to 3-year band region shows an in-phase relationship between summertime runoff and EASM indices. An anti-phase relationship between summertime runoff and EASM indices is detected in the 10- to 11-year band region (Figure 4(a)). An in-phase relationship between summertime runoff and SASM indices is detected in the 1- to 5-year band region around 1990–1996 (Figure 4(b)).

Wavelet coherence results show a coherence phase in the 3- to 5-year band around 1986–1995 and 2000–2005. These regions show an in-phase relationship between summertime runoff and EASM indices (Figure 4(c)). From 1990 to 1998, an in-phase relationship between summertime runoff and SASM indices is detected in the 2- to 6-year band (Figure 4(d)).

Cross-wavelet power spectra of summertime runoff at Yichang hydrological station and EASM indices show a significant power in the 1- to 3-year band around 1992–2000. The anti-phase relationship in the region is illustrated in Figure 5(a). The cross-wavelet power spectra of summertime runoff at Yichang hydrological station and SASM indices show a significant power in the 1- to 3-year band around 1965–1972 and 1992–1998. An in-phase relationship occurs around 1965–1972, and an anti-phase relationship occurs around 1992–1998 (Figure 5(b)).

The wavelet coherence of summertime runoff and EASM indices shows a 1- to 5-year band around 1980–1990 and 1992–1998. These regions show anti-phase relationships between summertime runoff and EASM indices. An in-phase relationship between summertime runoff and EASM indices is detected in the 4- to 7-year band around 1965–1975 (Figure 5(c)). The wavelet coherence of summertime runoff and SASM indices shows the 1- to 6-year band around 1963–1971 (in-phase relationship), 1980–1990 (in-phase relationship), and 1991–2002 (anti-phase relationship) (Figure 5(d)).

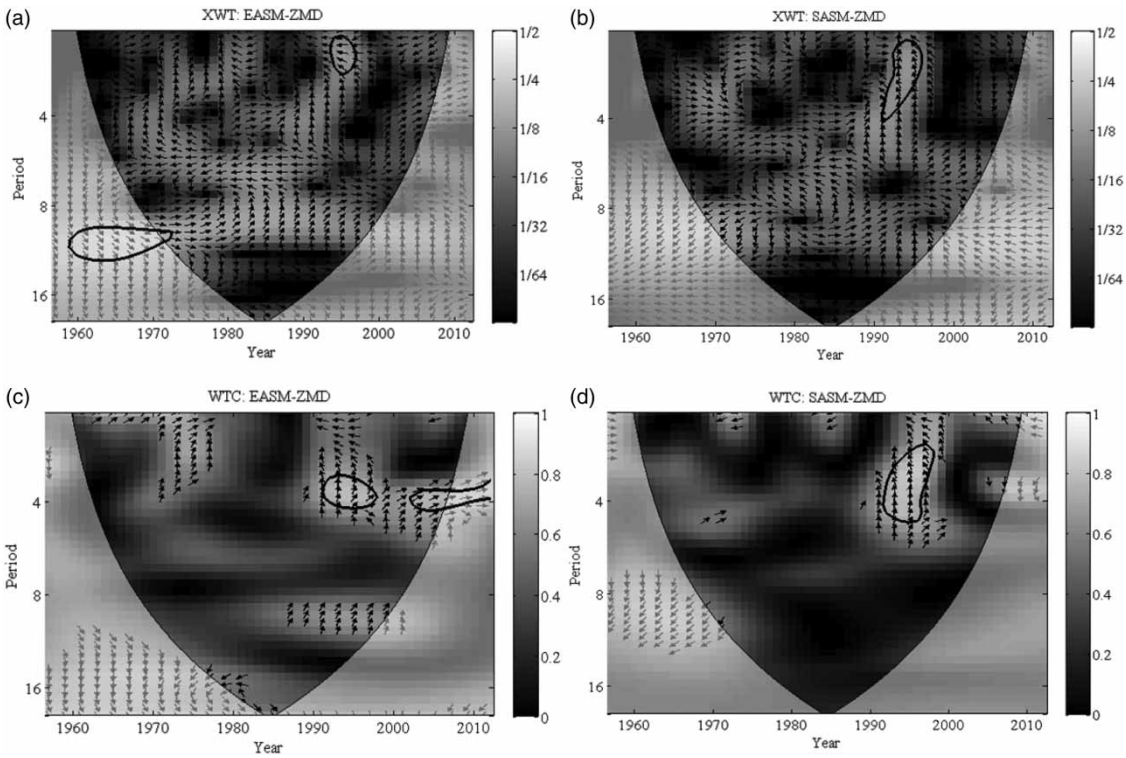

Figure 4 | Cross-wavelet and wavelet coherence spectra of summertime runoff and Asian summer monsoon indices at Zhimenda hydrological station during 1957–2012. The relative phase relationships between the two time series are shown as arrows (with in-phase pointing right, anti-phase pointing left).

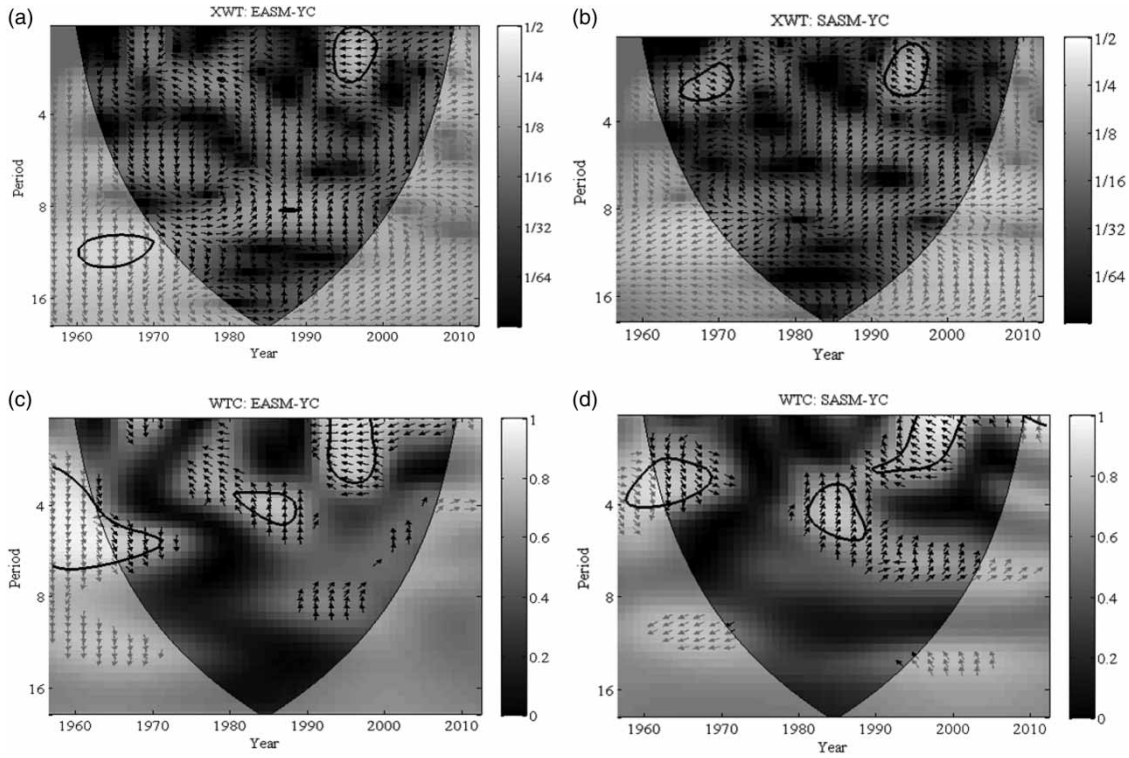

Figure 5 | Cross-wavelet and wavelet coherence spectra of summertime runoff and Asian summer monsoon indices at Yichang hydrological station during 1957–2012. The relative phase relationships between the two time series are shown as arrows (with in-phase pointing right, anti-phase pointing left).

In the middle reaches of the Yangtze River basin, significant power in the 1- to 3-year band around 1978–1980 and 1993–1996 is detected in the cross-wavelet power spectra. An anti-phase relationship between summertime runoff and EASM indices is seen in these regions. The 6- to 10-year band around 1981–1992 also has a significant power. The phase relationships between summertime runoff and EASM indices are unstable in this region, and have in-phase and anti-phase components simultaneously (Figure 6(a)). In other research, a similar situation was detected between maximum streamflow and other large-scale circulation patterns at Hankou hydrological station (Zhang *et al.* 2007). The cross-wavelet power spectra of summertime runoff and SASM indices show a significant power in the 1- to 3-year band around 1963–1975 and 1994–1996. Summertime runoff and SASM indices in these regions show an in-phase relationship around 1963–1975, and an anti-phase relationship around 1994–1996 (Figure 6(b)).

Wavelet coherence results show a coherence phase in the 5- to 12-year band around 1963–1973 and 1990–2005. Phase relationships between summertime runoff and EASM indices are unstable in these regions. There is also an anti-phase relationship between summertime runoff and EASM indices in the 1- to 4-year band around 1969–1995 (Figure 6(c)). A coherence phase in the 2- to 5-year band around 1961–1969 is detected in the wavelet coherence power spectra of summertime runoff and SASM indices. There is an in-phase relationship in this region (Figure 6(d)).

Figure 7(a) illustrates the cross-wavelet power spectra of summertime runoff at Datong station and EASM indices. The results indicate there is a significant power in the 1- to 3-year band around 1979–1982. An anti-phase relationship exists in the region. There is also a significant power in the 6- to 10-year band around 1981–1990. The phase relationship is unstable in this region. The cross-wavelet power spectra of summertime runoff and SASM indices show a significant power in the 1- to 3-year band around 1963–1979. An in-phase relationship exists in this region (Figure 7(b)).

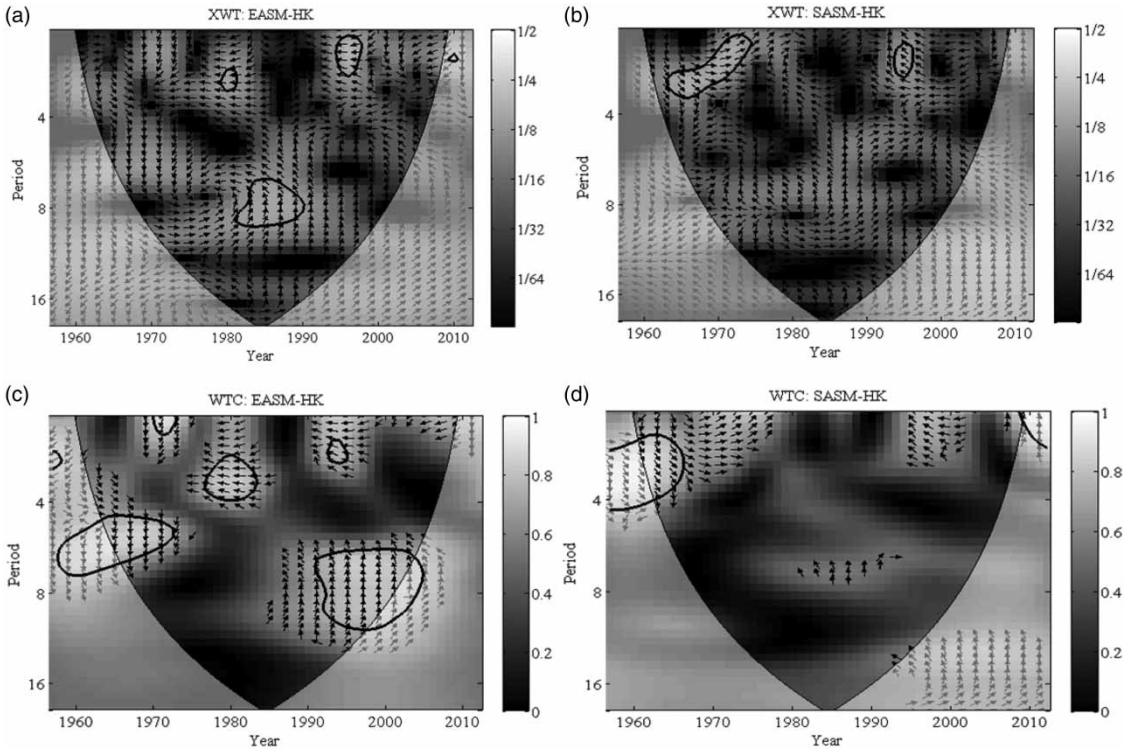

Figure 6 | Cross-wavelet and wavelet coherence spectra of summertime runoff and Asian summer monsoon indices at Hankou hydrological station during 1957–2012. The relative phase relationships between the two time series are shown as arrows (with in-phase pointing right, anti-phase pointing left).

Coherence phases in the 1- to 6-year band around 1963–1973, 1978–1985, and 1991–1993 are detected in the wavelet coherence power spectra. The phase relationships between summertime runoff and EASM indices during 1963–1973 are unstable. Phase relationships during 1978–1985 and 1991–1993 are anti-phase. There is also a coherence phase in the 5- to 12-year band around 1989–2005. The phase relationships between summertime runoff and EASM indices are unstable in this region (Figure 7(c)). The wavelet coherence of summertime runoff and SASM indices show there is a coherence phase in the 1- to 5-year band around 1962–1964 and 1970–1978. The phase relationships during 1962–1964 and 1970–1978 are in-phase (Figure 7(d)).

DISCUSSION

In the source and upper regions of the Yangtze River basin, a relatively large area exhibits phase relationships between summertime runoff and SASM indices (Figures 4 and 5). In the midstream and downstream regions of the Yangtze River basin, a relatively large area exhibits phase relationships between summertime runoff and EASM indices (Figures 6 and 7). These results indicate that summertime runoff of the source and upper regions of the Yangtze River basin is mainly influenced by the SASM. Summertime runoff of the midstream and downstream regions of the Yangtze River basin is controlled by EASM. Previous research confirmed that the meridional water vapor fluxes carried by the EASM are dominant in the midstream and downstream regions of the Yangtze River basin. In contrast, the zonal water vapor fluxes are relatively large in the source and upper regions of the Yangtze River basin (Huang *et al.* 2012).

The wind field characteristics at the 850 hPa geopotential height associated with the Asian summer monsoons can provide insights into the formation and generation of precipitation and streamflow in the Yangtze River basin (Zhang *et al.* 2008). Exploring the summertime wind field characteristics at the 850 hPa geopotential height can therefore facilitate the understanding of the impacts of

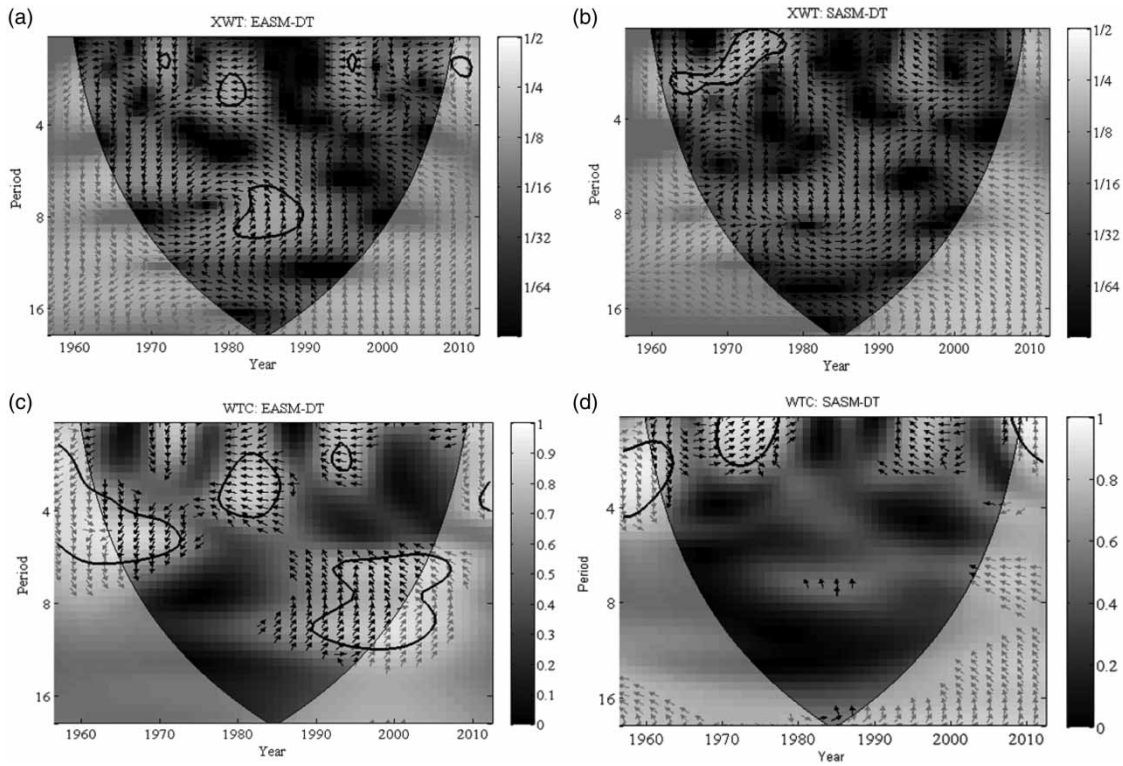

Figure 7 | Cross-wavelet and wavelet coherence spectra of summertime runoff and Asian summer monsoon indices at Datong hydrological station during 1957–2012. The relative phase relationships between the two time series are shown as arrows (with in-phase pointing right, anti-phase pointing left).

Asian summer monsoons on runoff in the Yangtze River basin.

A summertime wind field characteristics map in the Yangtze River basin confirms the deductions about the regional differences in the relationships between the summer runoff and Asian summer monsoons. As shown in Figure 8, vector arrows of the wind field indicate a southwest airflow field in the source and upper regions of the Yangtze River basin. The prevailing winds in these regions blow from the southwest. The SASM brings the southwest airflow into the source and upper regions of the Yangtze River basin (Chen 2013; Wei *et al.* 2014), and forms the regional dominant airflow direction and water vapor source. Therefore, changes of the SASM will be a key factor affecting the formation and generation of summertime precipitation and runoff in the source and upper regions of the Yangtze River basin. The prevailing winds in the midstream and downstream regions of the Yangtze River basin blow from the east. The EASM forms the regional dominant airflow direction and water vapor source in the midstream and downstream regions of the Yangtze River basin (Zhang *et al.* 2008, 2012). Therefore, the EASM will be a key factor affecting the formation and generation of summertime precipitation and runoff in the midstream and downstream regions of the Yangtze River basin.

Table 2 illustrates the phase relationships between summertime runoff and Asian summer monsoons in the Yangtze River basin during 1957–2012. Generally, an anti-phase relationship between summertime runoff and EASM indices dominates in the midstream and downstream regions of the Yangtze River basin (Figures 6 and 7). In these regions, variations of the EASM will result in floods and droughts (Li & Zeng 2002; Qian *et al.* 2003; Wang & Zhou 2005). In the source region of the Yangtze River basin, an in-phase relationship is detected between summertime runoff and SASM indices. Phase relationships are ambiguous, and have in-phase and anti-phase relationships simultaneously.

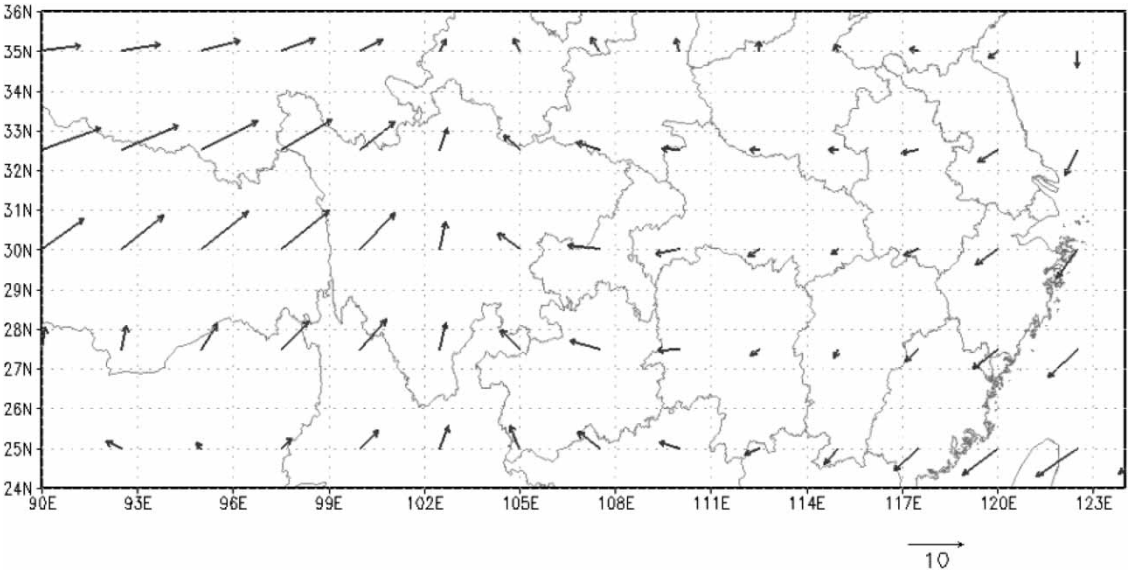

Figure 8 | Summertime wind field characteristics at 850 hPa geopotential height in the Yangtze River basin during 1957–2012.

Table 2 | Phase relationships between summertime runoff and Asian summer monsoons in the Yangtze River basin during 1957–2012

Stations	Location	Relationships with Asian summer monsoons
Zhimenda	Source region	Mainly anti-phase relationships with SASM
Yichang	Upper region	Anti-phase and in-phase relationships with SASM
Hankou	Midstream region	Mainly anti-phase relationships with EASM
Datong	Downstream region	Mainly anti-phase relationships with EASM

CONCLUSIONS

Research on the summertime runoff variations and their connections with Asian summer monsoons in the Yangtze River basin can give insights for explanation of the regional change patterns of hydrological processes and climate change. With the help of continuous wavelet transform, cross-wavelet, and wavelet coherence analysis methods, this research explored summertime runoff variations and their connections with Asian summer monsoons during 1957–2012 in the Yangtze River basin. The following conclusions were drawn:

- There are obvious regional differences in periodical characteristics of summertime runoff in the Yangtze River basin. The 1- to 3-year band power spectra are detected in the summertime runoff in the source and upper regions of the Yangtze River basin. In the midstream and downstream regions, the 7- to 10-year band power spectra are detected in the summertime runoff.
- The SASM brings the southwest airflow into the source and upper regions of the Yangtze River basin, and forms the regional dominant airflow direction and water vapor source, while the EASM forms the regional dominant airflow direction and water vapor source in the midstream and downstream regions of the Yangtze River basin.
- In-phase relationships between summertime runoff and SASM indices are detected in the source region of the Yangtze River basin. Anti-phase relationships between summertime runoff and EASM indices dominate in the midstream and downstream regions of the Yangtze River basin. Phase relationships between summertime runoff and Asian summer monsoons are ambiguous in the upper region of the Yangtze River basin.

Although our research findings can provide insights for improving water resources management and hydrological hazards mitigation in the Yangtze River basin, there

remain some shortcomings. The relationships between runoff and Asian summer monsoons are complicated. Many large-scale atmospheric systems play important roles in affecting the hydrological processes in the Yangtze River basin, and thus increase the noise in the linkages between runoff and Asian summer monsoons. Quantitative exploration of the mechanisms behind the connections between runoff and Asian summer monsoons in the Yangtze River basin is still required in future research.

ACKNOWLEDGEMENTS

This study was supported and funded by the National Natural Science Foundation of China (Grants No. 51609008), the Natural Science Foundation of Hubei Province (No. 2016CFA092), and the Fundamental Research Funds for Central Public Welfare Research Institutes (No. CKSF2015015/SH), and China CDM Fund Project (Grants No. 2012044).

REFERENCES

Adamowski, J. & Prokoph, A. 2014 Determining the amplitude and timing of streamflow discontinuities: a cross wavelet analysis approach. *Hydrol. Process.* **28**, 2782–2793.

Blender, R., Zhu, X. H., Zhang, D. & Fraedrich, K. 2011 Yangtze summer runoff, precipitation, and the East Asian monsoon in a 2800 years climate control simulation. *Quat. Int.* **244**, 194–201.

Chen, J. 2013 Water cycle mechanism in the source region of Yangtze River. *J. Yangtze River Sci. Res. Inst.* **30** (7), 1–6 (in Chinese).

Clift, P. D., Hodges, K. V., Heslop, D., Hannigan, R., Van Long, H. & Calves, G. 2008 Correlation of Himalayan exhumation rates and Asian monsoon intensity. *Nat. Geosci.* **1**, 875–880.

Cuo, L., Zhang, Y. X., Zhu, F. X. & Liang, L. Q. 2014 Characteristics and changes of streamflow on the Tibetan plateau: a review. *J. Hydrol. Reg. Stud.* **2**, 49–68.

Ding, Y. H. & Chan, J. C. L. 2005 The East Asian summer monsoon: an overview. *Meteorol. Atmos. Phys.* **89**, 117–142.

Ding, Y. H., Sun, Y., Liu, Y. Y., Si, D., Wang, Z. Y., Zhu, Y. X., Liu, Y. J., Song, Y. F. & Zhang, J. 2013 Interdecadal and interannual variabilities of the Asian summer monsoon and its projection of future change. *Chin. J. Atmos. Sci.* **37** (2), 253–280 (in Chinese).

Farge, M. 1992 Wavelet transforms and their applications to turbulence. *Annu. Rev. Fluid Mech.* **24** (1), 395–458.

Gebregiorgis, D., Hathorne, E. C., Sijinkumar, A. V., Nath, B. N., Nürnberga, D. & Franka, M. 2016 South Asian summer monsoon variability during the last ~54 kyrs inferred from surface water salinity and river runoff proxies. *Quat. Sci. Rev.* **138**, 6–15.

Grinsted, A., Moore, J. C. & Jevrejeva, S. 2004 Application of the cross wavelet transform and wavelet coherence to geophysical time series. *Nonlinear Process. Geophys.* **11**, 561–566.

Han, L. F., Xu, Y. P., Pan, G. B., Deng, X. J., Hu, C. S., Xu, H. L. & Shi, H. Y. 2015 Changing properties of precipitation extremes in the urban areas, Yangtze River Delta, China, during 1957–2013. *Nat. Hazards* **79** (1), 437–454.

Huang, R. H., Chen, J. L., Wang, L. & Lin, Z. D. 2012 Characteristics, processes, and causes of the spatio-temporal variabilities of the East Asian monsoon system. *Adv. Atmos. Sci.* **29**, 910–942.

Ionita, M., Lohmann, G., Rimbu, N. & Chelcea, S. 2012 Interannual variability of Rhine River streamflow and its relationship with large-scale anomaly patterns in spring and autumn. *J. Hydrometeorol.* **13** (1), 172–188.

Kitoh, A. 2004 Effects of mountain uplift on East Asian summer climate investigated by a coupled atmosphere–ocean GCM. *J. Clim.* **17**, 783–802.

Kubota, Y., Tada, R. & Kimoto, K. 2015 Changes in East Asian summer monsoon precipitation during the Holocene deduced from a freshwater flux reconstruction of the Changjiang (Yangtze River) based on the oxygen isotope mass balance in the northern East China Sea. *Clim. Past* **11**, 265–281.

Kulkarni, M. A., Singh, A. & Mohanty, U. C. 2012 Effect of spatial correlation on regional trends in rain events over India. *Theor. Appl. Climatol.* **109**, 497–505.

Kurita, N., Fujiyoshi, Y., Nakayama, T., Matsumi, Y. & Kitagawa, H. 2015 East Asian monsoon controls on the inter-annual variability in precipitation isotope ratio in Japan. *Clim. Past* **11**, 339–353.

Labat, D. 2005 Recent advances in wavelet analyses: part 1. A review of concepts. *J. Hydrol.* **314**, 275–288.

Latt, Z. Z. & Wittenberg, H. 2015 Hydrology and flood probability of the monsoon-dominated Chindwin River in northern Myanmar. *J. Water Clim. Change* **6** (1), 144–160.

Lee, J. Y., Wang, B., Wheeler, M. C., Fu, X., Waliser, D. E. & Kang, I. S. 2013 Real-time multivariate indices for the boreal summer intraseasonal oscillation over the Asian summer monsoon region. *Clim. Dyn.* **40**, 493–509.

Li, J. P. & Zeng, Q. C. 2002 A unified monsoon index. *Geophys. Res. Lett.* **29** (8). doi: 127410.1029/2001GL013874.

Li, J. P., Wu, Z. W., Jiang, Z. H. & He, J. H. 2010 Can global warming strengthen the East Asian summer monsoon? *J. Clim.* **23**, 6696–6705.

Li, F. X., Chen, D., Tang, Q. H., Li, W. H. & Zhang, X. J. 2016 Hydrological response of east China to the variation of East Asian summer monsoon. *Adv. Meteorol.* doi:10.1155/2016/4038703.

Li, F. X., Zhang, S. Y., Chen, D., He, L. & Gu, L. L. 2017 Inter-decadal variability of the east Asian summer monsoon and its impact on hydrologic variables in the Haihe River basin, China. *J. Resour. Ecol.* **8** (2), 174–184.

Qian, Y. F., Zheng, Y. Q., Zhang, Y. & Miao, M. Q. 2003 Responses of China's summer monsoon climate to snow anomaly over the Tibetan Plateau. *Int. J. Climatol.* **23**, 593–613.

Sang, Y. F. 2013 A review on the applications of wavelet transform in hydrology time series analysis. *Atmos. Res.* **122**, 8–15.

Schiemann, R., Glazirina, M. G. & Schär, C. 2007 On the relationship between the Indian summer monsoon and river flow in the Aral Sea basin. *Geophys. Res. Lett.* **34**, L05706.

Shan, L. J., Zhang, L. P., Xiong, Z., Chen, X. C., Chen, S. D. & Yang, W. 2017 Spatio-temporal evolution characteristics and prediction of dry–wet abrupt alternation during the summer monsoon in the middle and lower reaches of the Yangtze River Basin. *Meteorol. Atmos. Phys.* 1–14. doi: 10.1007/s00703-017-0528-7.

Singh, D., Tsiang, M., Rajaratnam, B. & Diffenbaugh, N. S. 2014 Observed changes in extreme wet and dry spells during the South Asian summer monsoon season. *Nat. Clim. Change* **4**, 456–461.

Steirou, E., Gerlitz, L., Apel, H. & Merz, B. 2017 Links between large-scale circulation patterns and streamflow in Central Europe: a review. *J. Hydrol.* **549**, 484–500.

Tamaddun, K. A., Kalra, A. & Ahmad, S. 2017 Wavelet analyses of western US streamflow with ENSO and PDO. *J. Water Clim. Change* **8** (1), 26–39.

Thomas, T., Gunthe, S. S., Ghosh, N. C. & Sudheer, K. P. 2015 Analysis of monsoon rainfall variability over Narmada basin in central India: implication of climate change. *J. Water Clim. Change* **6** (3), 615–627.

Torrence, C. & Compo, G. P. 1998 A practical guide to wavelet analysis. *Bull. Am. Meteorol. Soc.* **79**, 61–78.

Torrence, C. & Webster, P. J. 1998 The annual cycle of persistence in the El Nino/Southern Oscillation. *Q. J. R. Meteorol. Soc.* **124** (550), 1985–2004.

Turner, A. G. & Annamalai, H. 2012 Climate change and the South Asian summer monsoon. *Nat. Clim. Change* **2**, 587–595.

Wang, Y. Q. & Zhou, L. 2005 Observed trends in extreme precipitation events in China during 1961–2001 and the associated changes in large-scale circulation. *Geophys. Res. Lett.* **32**, L09707.

Wei, W., Chang, Y. P. & Dai, Z. J. 2014 Streamflow changes of the Changjiang (Yangtze) River in the recent 60 years: impacts of the East Asian summer monsoon, ENSO, and human activities. *Quat. Int.* **336**, 98–107.

Wu, G. X., Liu, Y. M., He, B., Bao, Q., Duan, A. M. & Jin, F. F. 2012 Thermal controls on the Asian summer monsoon. *Sci. Rep.* **404**. doi: 10.1038/srep00404.

Yang, Z. S., Wang, H. J., Saito, Y., Milliman, J. D., Xu, K., Qiao, S. & Shi, G. 2006 Dam impacts on the Changjiang (Yangtze) River sediment discharge to the sea: the past 55 years and after the Three Gorges Dam. *Water Resour. Res.* **42**, W04407. doi: 10.1029/2005WR003970.

Zeng, G., Wang, W. C., Shen, C. M. & Hao, Z. X. 2014 Summer precipitation changes over the Yangtze River Valley and North China: simulations from CMIP3 models. *Asia Pac. J. Atmos. Sci.* **50**, 355–364.

Zhang, Q., Xu, C. Y., Jiang, T. & Wu, Y. 2007 Possible influence of ENSO on annual maximum streamflow of the Yangtze River, China. *J. Hydrol.* **333**, 265–274.

Zhang, Q., Xu, C. Y., Zhang, Z. X., Chen, Y. D., Liu, C. L. & Lin, H. 2008 Spatial and temporal variability of precipitation maxima during 1960-2005 in the Yangtze River basin and possible association with large-scale circulation. *J. Hydrol.* **353**, 215–227.

Zhang, E. F., Savenije, H. H. G., Chen, S. L. & Mao, X. H. 2012 An analytical solution for tidal propagation in the Yangtze Estuary, China. *Hydrol. Earth Syst. Sci.* **16**, 3327–3339.

First received 23 September 2016; accepted in revised form 1 October 2017. Available online 30 October 2017